DOI: 10.1002/ejoc.200600897

NMR Investigation of the Bound Conformation of Natural and Synthetic Oligomannosides to Banana Lectin

Caroline Clavel,[a] Angeles Canales,[b] Garima Gupta,[c] F. Javier Cañada,[b] Soledad Penadés,*[a] Avadhesha Surolia,*[c,d] and Jesús Jiménez-Barbero*[b]

Keywords: Mannose oligosaccharides / NMR spectroscopy / Molecular dynamics / Banana lectin / Molecular recognition

The conformational behaviour of three mannose-containing oligosaccharides, namely, the α1→3[α1→6] trisaccharide, a heptasaccharide with α1→2, α1→3 and α1→6 linkages and a tetrasaccharide consisting of α1→3 and α1→2 linkages, when bound to banana lectin (BanLec) has been evaluated by trNOE NMR methods and docking calculations. It was found that the molecular recognition event involves a conformational selection process with only one of the conformations present in the free state of the sugar being recognised at the lectin binding site.

Introduction

The recognition of high-mannose-type oligosaccharides plays a key role in protein quality control, with several intracellular proteins, such as lectins, chaperones and glycan-processing enzymes, being involved in this process.[1,2] A number of proteins bind the high-mannose saccharides found on the surface of the HIV-associated envelope glycoprotein gp120, thus interfering with the viral life cycle, providing a putative manner of controlling a variety of infections, including HIV.[3] These proteins are thought to recognise high-mannose-type glycans with subtly different structures, although the precise specificities are yet to be clarified. In order to gain a better understanding of these protein–carbohydrate recognition events and as a key step for controlling them, access to well-defined mannose-containing oligosaccharides by means of organic synthesis methods is of paramount importance.[4,5] In addition, the possibility for these oligosaccharides to be part of saccharide-containing clusters is also highly desirable.[6] Indeed, it has been demonstrated that synthetic oligomannose clusters could mimic some of these carbohydrate epitopes (also including those of the 2G12 antibody), providing antigenicity.[7] Recently, gold glyconanoparticles (GNPs) have been designed and used as new multivalent tools that mimic glycoconjugate presentation on the cell surface. As key advantages, GNPs are highly soluble under physiological conditions, stable against enzymatic degradation and, more importantly, they are essentially non-toxic.[8] Therefore, GNPs may be used as suitable tools for basic studies of carbohydrate interactions and for intervention related to key biological processes.[9]

The precise three-dimensional structure and dynamics of the saccharides have important implications in these recognition events and, thus, an understanding of these particular aspects is crucial for controlling the recognition events.[10] Herein, as part of a project devoted to the synthesis, interaction studies and applications of gold glyconanoparticles,[11] we present the study of the banana lectin bound geometries of three linear and branched oligomannosides containing 1→2, 1→3 and 1→6 linkages. These molecules have been prepared as components of mannose-containing GNPs as potential microbicides that could block HIV-1 gp120 binding to DC-SIGN. We have decided to use banana lectin (BanLec) as the model lectin. BanLec is a dimeric plant lectin from the jacalin-related lectin family.[12] It is widely recognized that plant lectins are excellent model systems for the study of protein–carbohydrate interactions because of their robustness and ready availability.[13] Moreover, it has been speculated that lectins of the jacalin family are involved in interactions with the gp120 glycoprotein.[3]

Results and Discussion

The three oligosaccharides studied herein show structural features also present in the $Man_9GlcNAc_2$ oligosaccharide, although they may be considered as fragments or non-natural modifications thereof. Therefore, experimental

[a] Grupo de Carbohidratos, IIQ-CSIC,
Américo Vespucio 49, 41092 Sevilla, Spain
E-mail: penades@iiq.csic.es
[b] CIB-CSIC,
Ramiro de Maeztu 9, 28040 Madrid, Spain
E-mail: jjbarbero@cib.csic.es
[c] Indian Institute of Science,
Bangalore 560012, India
[d] National Institute of Immunology,
New Delhi 110067, India
E-mail: surolia@mbu.iisc.ernet.in
Supporting information for this article is available on the WWW under http://www.eurjoc.org or from the author.

data on the structure and conformational behaviour of the natural complete oligosaccharide and fragments thereof are available from previous X-ray crystallographic and NMR spectroscopic studies.[14,15] Computational studies using molecular mechanics and dynamics simulations have also been described for the (1→2)- and (1→6)-linked trimannoside.[16] These latter studies suggested little correlation between the motion of the two glycosidic linkages, (1→2) and (1→6), which indeed behaved as they do in the corresponding (1→2)- and (1→6)-linked dimannosides.[17] Therefore, analyses of the tetra- (**1**), tri- (**2**) and heptasaccharides (**3**) will be described independently.

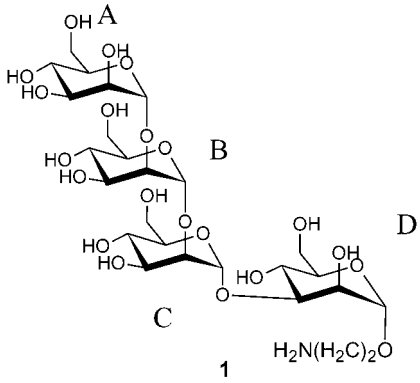

1

Tetrasaccharide 1

The conformational analysis of this molecule in the free state was evaluated by using NOE-based NMR experiments and molecular mechanics and dynamics calculations.[18] Its conformational behaviour may be described by a distribution of conformers that display *exo* anomeric conformations around all the torsion angles Φ of the molecule and fluctuations around negative and positive values of the Ψ aglyconic linkages. A superimposition of the different representative conformers is given in Figure 1.

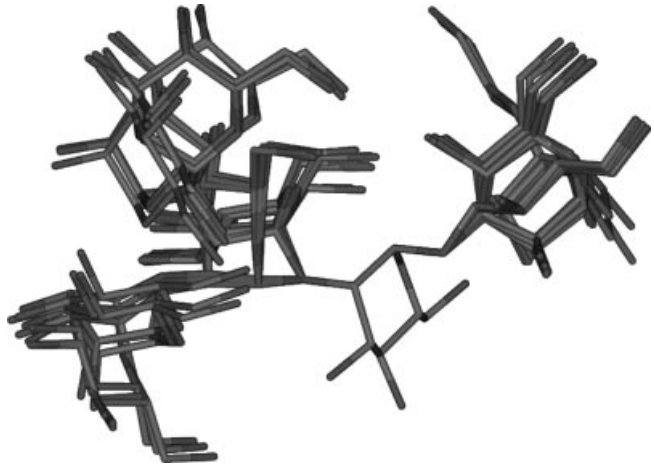

Figure 1. Superimposition of the major conformers of **1** in the free state according to MM3* calculations. The 1→3-linked residue has been chosen for the superimposition.

In particular, the positive and negative regions of Ψ are both represented in available X-ray structures of mannose oligosaccharides and account for the set of three NOE contacts typically observed across this glycosidic linkage.[19] For the Manα1→2Man linkage, the H1–H1′ contact can only arise from positive Ψ conformers and the H5′–H1 contact only from negative Ψ geometries. The interglycosidic H1′–H2 pair is at an NOE distance in both conformations. For the Manα1→3Man glycosidic linkage, the H2–H5′ contact may be observed for both positive and negative Ψ geometries, but should be stronger for the latter arrangement. Finally, the H1′–H2 linkage (see Figure 1 of the Supporting Information) can only arise from positive Ψ geometries. The interglycosidic H1′–H3 pair is again at an NOE distance in both conformations.

Tetrasaccharide **1** displays two Manα1→2Man linkages, dubbed ManAα1→2ManB and ManBα1→2ManC. In the free state, a 30:70 distribution between the positive and negative Ψ conformers for each Manα1→2Man or Manα1→3Man glycosidic linkage quantitatively accounts for the observed NOEs.

As mentioned in the Introduction, BanLec was chosen as the model lectin to test the interaction abilities of these

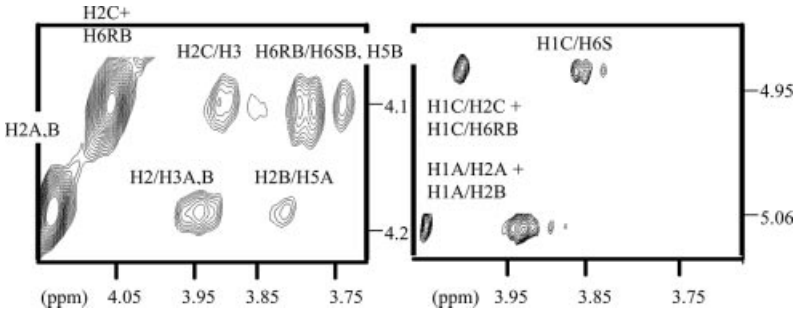

Figure 2. The binding of **2** to banana lectin as monitored by NMR spectroscopy. The figure shows sections of the anomeric region (right) and H2 region (left) of the trNOESY spectrum (250 ms) of **1** in the presence of banana lectin (30:1 molar ratio). Cross peaks show the same sign as diagonal peaks, indicating binding. Key trNOEs are indicated.

Table 1. Calculated and experimental interproton distances [Å] for **1** and the observed NOE contacts.

Linkage	Proton pair	Exp. distances in the bound state (CORCEMA)[a,b]	Exp. distances in the free state[a,c]	trNOE intensity[d]	Distance[e] for conformers: positive Ψ/negative Ψ
α1→2	H1′–H1	AB 3.4	AB 3.2	weak	2.6–3.4/4.1–4.4
	H1′–H1	BC 3.4	BC 3.3	weak	
	H1′–H2	AB 2.55	AB 2.4	strong	2.1–2.3/2.3–2.6
	H1′–H2	BC 2.55	BC 2.4	strong	
	H5′–H1	AB 2.35	AB 2.5	strong-medium	2.4–3.0/2.3–2.9
	H5′–H1	BC 2.35	BC 2.5	strong-medium	
	H5′–H2	not detected	not detected	not detected	4.4/3.0
α1→3	H1′–H3	CD 2.3	CD 2.3	strong	2.2/2.5
	H1′–H2	CD 3.1	CD 3.0	weak	2.6/4.2
	H5′–H2	CD 2.4	CD 2.5	medium	2.8/2.4

[a] AB and BC represent the two Manα1→2Man linkages, while CD refers to the Manα1→3Man linkage of **1**. In all cases, the corresponding non-reducing moiety of a given linkage is primed. [b] The first column of data gathers the averaged interproton distances calculated by the CORCEMA analysis of the trNOE cross peaks at four mixing times. [c] Distances for compound **1** in the free state were derived from 1D and 2D NOESY and T-ROESY data by using the isolated spin–pair approximation (ISPA), according to the protocol described in the Exp. Sect. Error estimation in the measurement is less than 0.2 Å. [d] Experimental trNOESY intensities as deduced from intensity volume measurement. [e] Estimated distances for the representative conformers of both Manα1→2Man and Manα1→3Man linkages in the positive Ψ and negative Ψ regions.

oligosaccharides as its 3D structure when complexed with mannose and other saccharides has recently been reported.[20,21] The addition of this lectin to NMR tubes containing **1** induced broadening of its NMR signals (Figure 2).[22]

Saturated transfer difference (STD) is also a straightforward NMR method that permits ligand binding to receptors to be determined.[23,24] Thus, STD experiments were used to further study the interaction, as also depicted in Figure 1 of the Supporting Information. For **1**, clear STD effects for all the H2 protons were deduced by visual inspection, the STD effects being smaller for the anomeric signals.

trNOE experiments were then used to deduce the conformation of the saccharide bound to the lectin.[22,24–26] As previously shown, for ligands that are not bound tightly and for which exchange between the free and bound states occurs at a reasonably fast rate, the transferred nuclear Overhauser enhancement (trNOESY) experiment provides an adequate means for determining the conformation of the bound ligand.[22,26] In the bound state, strong and negative NOE cross peaks were observed for **1** in the presence of the lectin at a 20:1 ligand/receptor molar ratio, even at short mixing times (Figure 2 of the Supporting Information). This observation contrasts with findings noted for the free state, for which NOE cross peaks were weakly positive and clearly indicates sugar recognition by the lectin (Table 1).

A CORCEMA-based full-relaxation matrix analysis[27] of the cross peaks was performed to deduce the experimental proton–proton distances in the bound state, which were then compared with those estimated for the free sugar. For both Manα1→2Man linkages, the H1′–H1 and H1′–H2 cross peaks were weaker in the bound than in the free state, while the H5′–H1 and H5′–H2 ones were stronger. These observations are in agreement with a shift in the conformational distribution towards negative Ψ angles. Similar behaviour was deduced for the Manα1→3Man linkage. In this case the H1′–H2 and H5′–H2 cross peak intensities in the bound state relative to those of the free one agree with a significant population of the negative Ψ region, whereas a strong H1′–H3 contact does not allow discrimination between the positive and negative regions. Therefore, the lectin modifies the conformational equilibrium of **1**, shifting the conformational populations. According to the NOE data, the tetrasaccharide still retains a certain conformational mobility, but there is a high predominance of negative conformers for the $\Psi_{1\rightarrow2}$ torsion angles and positive ones for the $\Psi_{1\rightarrow3}$ torsion angles (above 80%), as depicted in Figure 3 of the Supporting Information.

Trisaccharide 2

The conformational behaviour of this trisaccharide in the free state and bound to different lectins has been extensively studied.[28–32] The results indicate that there is a single conformation for the *exo* anomeric torsion angle Φ, centred around –60°, with the concomitant presence of conformational mobility around the $\omega_{1\rightarrow6}$ torsion (equilibrium between the gg and gt conformers) with additional more restricted fluctuations around $\Psi_{1\rightarrow3}$. Thus, the combination of these degrees of freedom covers the conformational space available to **2**.

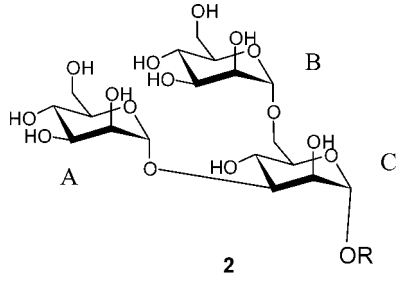

2

For trisaccharide **2**, major STDs (Figure 4 of the Supporting Information) are observed for both H2 signals of the external residues as well as a minor effect for H6R of B and/or H2 of C. This pattern seems to indicate major recognition of the 1→3 arm.

Table 2. Calculated and experimental interproton distances [Å] for **2** and the observed NOE contacts.

Linkage	Proton pair	Exp. distances in the bound state (CORCEMA)[a,b]	trNOESY intensity[c]	Distance for conformers: positive Ψ/negative Ψ[d]
α1→3	H_1'–H_3	AB 2.4	strong	2.1/2.5
	H_1'–H_2	AB overlap	weak	2.5/4.3
	H_5'–H_2	AB 2.5	medium	3.2/2.3
α1→6	H_1'–H_{6R}	CB 2.4	strong	2.4–2.7
	H_1'–H_{6S}	CB 2.9	weak	2.9–3.5
	H_4–H_{6R}	>3.1	very weak	N.a.
	H_1'–H_5	CB not detected	not detected	4.2–4.7

[a] AB represents the Manα1→3Man linkage, while CB refers to the Manα1→6Man linkage. In all cases, the corresponding non-reducing moiety of a given linkage is primed. For the Manα1→6Man linkage, only Ψ = 180° is considered. [b] The first column of data gathers the averaged interproton distances calculated from the CORCEMA analysis of the trNOE cross peaks at four mixing times. Error estimation in the measurement is less than 0.2 Å. [c] Experimental trNOESY intensities as deduced from intensity volume measurement. [d] Estimated distances for representative conformers of both Manα1→3Man and Manα1→6Man linkages in the positive Ψ and negative Ψ regions.

The trNOESY experiments (Figure 2) provided interatomic distances for the key proton pairs of all the linkages, as reported in Table 2. For the (1→3) linkage,[28] the H1′–H3 NOE does not permit differentiation between the positive and negative Ψ regions. However, the relatively strong H5′–H2 cross peak indicates a major contribution of negative $\Psi_{1\rightarrow3}$ torsion angles in the bound state. For the (1→6) linkage no H1′–H5 cross peak was observed, thus indicating a major *anti* conformer around Ψ, also in agreement with the relative NOE values for the H1′–H6R and H1′–H6S proton pairs, which are similar to those observed for the free state. Moreover, the H4–H6R contact was very weak in the trNOESY spectrum, pointing towards the recognition of a major gg rotamer for the (1→6) linkage in the bound state, although binding of the gt geometry cannot be ruled out. According to these data, the lectin modifies the conformational equilibrium of **2**, shifting the conformational populations towards a major bound conformer,[33] as depicted in Figure 5 of the Supporting Information.

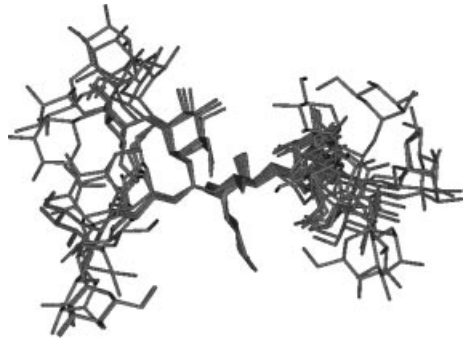

Figure 3. Conformational studies on **3**. The figure shows the superimposition of the representative geometries that encompass the possible conformational space available to free **3**. Calculations were run with MMOD 7.0, using MM3* and the GB/SA water solvation model.

Heptasaccharide 3

The heptasaccharide **3** shows two Manα1→2Manα1→2-Man branches that emanate from each terminal Man unit and which are also present in the trisaccharide **2**, as described above. Thus, this oligosaccharide may be described as a composition of **1** and **2**. Indeed, one of the arms of **3** corresponds exactly to tetrasaccharide **1**. The conformation of the free molecule was analysed (Table 3, Figure 3) through the use of MD simulations and NMR spectroscopic data (1D and 2D NOESY and T-ROESY).[18]

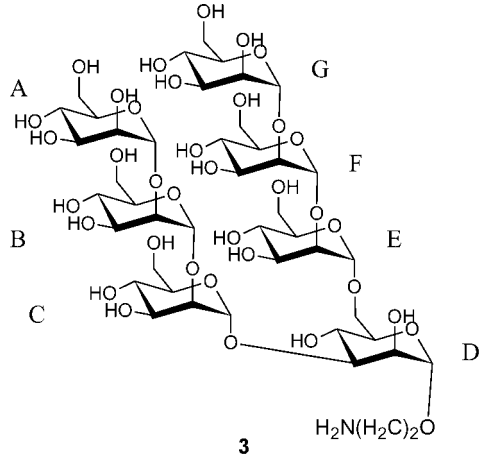

3

The negative Ψ conformation was in all cases preferred over the positive one, with a similar preference to that described above for free **1** (Figure 3).

Indeed, in the free state, for all Manα1→2Man linkages, the observed H5′–H1 NOE intensity was always significantly more intense (estimated distance 2.5 Å) than that observed for the corresponding H1′–H1 pair (estimated distance 3.3–3.4 Å).[18] The conformational equilibrium also favours negative over positive Ψ values around the ManCα1→3ManD linkage as the experimental average C1′–D2 distance was approximately 3.3 Å and that for C5′–D2 was 2.5 Å, closer to that expected for negative Ψ conformers. Thus, the conformational equilibrium in water favours negative Ψ conformers, with an estimated distribution of around 75:25.[18]

For the Manα1→6Man moiety again a basically pure Ψ *anti* conformation was predicted with the existence of both gg and gt rotamers around the C5–C6 bond of unit D.

Table 3. Calculated and experimental interproton distances [Å] for **3** and observed NOE contacts.

Linkage	Proton pair	Exp. distances in the bound state (CORCEMA)[a,b]	Exp. distances in the free state (ISPA model)[a,c]	trNOE intensity[d]	Distance[e] for conformers: positive Ψ/negative Ψ
α1→2	H1′–H1	AB >3.4	AB 3.3		2.6–3.4/4.1–4.3
	H1′–H1	BC >3.4	BC 3.3	not	
	H1′–H1	GF >3.4	GF 3.2	observed	
	H1′–H1	FE >3.4	FE 3.2		
	H1′–H2	AB 2.4	AB 2.4	strong	2.1–2.3/2.3–2.6
	H1′–H2	BC 2.3	BC 2.4	strong	
	H1′–H2	GF 2.4	GF 2.4	strong	
	H1′–H2	FE 2.3	FE 2.4	strong	
	H5′–H1	AB 2.9	AB 2.6	strong-medium	2.4–3.0/2.3–3.1
	H5′–H1	BC 2.9	BC 2.6	strong-medium	
	H5′–H1	GF 2.9	GF 2.6	strong-medium	
	H5′–H1	FE 2.8	FE 2.6	strong-medium	
α1→3	H1′–H3	CD 2.3	CD 2.3	strong	2.2/2.5
	H1′–H2	CD 3.4	CD 3.3	weak	2.6/4.2
	H5′–H2	CD 2.6	CD 2.5	medium	2.8/2.4
α1→6	H1′–H6a	ED 2.4	ED 2.4	strong	2.4–2.7
	H1′–H6b	ED 3.0	ED 2.9	weak	2.9–3.5
	H1′–H5	ED not detected	not detected	not detected	4.2–4.7

[a] AB, BC, GF and FE represent the α1→2 linkage, whereas CD and ED refer to α1→3 and α1→6 linkages, respectively. In all cases, the corresponding non-reducing moiety of a given linkage is primed. For the 1→6 linkage, only Ψ = 180° is considered. [b] The first column with data gathers the averaged interproton distances calculated from the CORCEMA analysis of the trNOE cross peaks at four mixing times. [c] Distances for compound **3** in the free state were derived using the isolated spin-pair approximation (ISPA) according to the protocol described in the Exp. Sect. from 1D and 2D NOESY and T-ROESY data. Error estimation in the measurement is less than 0.2 Å. [d] Experimental trNOESY intensities as deduced from intensity volume measurement. [e] Estimated distances for representative conformers of both Manα1→2Man and Manα1→3Man linkages in the positive Ψ and negative Ψ regions.

The STD for the heptasaccharide/BanLec sample (Figure 6 of the Supporting Information) again shows major enhancements for the H2 protons of the more external 1→2-linked residues and minor enhancements for the anomeric protons, although enhancements for the external protons as well as that of the 1→3-linked moiety are observable.

trNOESY experiments were also performed in order to further explore the binding features of **3** (Figure 4). Drastic differences are observed in the trNOESY spectrum of the heptasaccharide **3** in the presence of banana lectin. The H1′–H1 cross peaks essentially disappear for all 1→2 linkages, indicating a major shift of these linkages towards negative Ψ values. Moreover, the H5′–H1 cross peak also

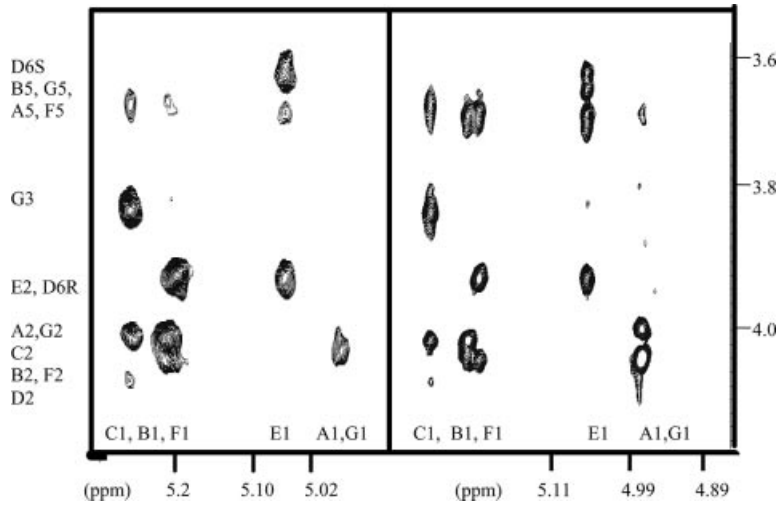

Figure 4. The binding of **3** to banana lectin as monitored by NMR spectroscopy. The figure shows sections of the anomeric region of the free state (right, ROESY, 400 ms mixing time) and bound state (left, trNOESY, 250 ms mixing time) of **3** in the presence of banana lectin (30:1 molar ratio). In the trNOESY, cross peaks show the same sign as diagonal peaks, indicating binding. Key trNOEs are indicated.

displays weaker intensities (vs. the intra-residue H1/H2 contacts) relative to those in the free state. This strongly restricts possible values of Φ and Ψ to around -30 ± 10 and -20 ± 10 for the 1→2 linkages. In this area, the H1′–H1 distances are larger than 4 Å, while the H5′–H1 distances are around 2.9 ± 0.2 Å, in agreement with the NMR experimental results.

For the 1→3 linkage, the bound conformer is not clearly defined and indeed the NOE data for the H1′–H3, H1′–H2, and H5′–H2 cross peaks are between those expected for the negative and positive Ψ regions. This probably means that this linkage retains a certain amount of conformational mobility in the bound state. A similar situation may be attributed to the intrinsically more flexible 1→6 linkage. In any case, the conformational mobility of the heptasaccharide is significantly reduced by the protein, especially for the four 1→2 linkages. A view of the putative bound conformers is shown in Figure 7 of the Supporting Information.

Docking Experiments

As a further step, and with this experimental information, 3D models of the possible complexes formed between **1**–**3** and banana lectin were built using both manual docking and AutoDock procedures. As mentioned before, BanLec was chosen as a model lectin.[20,21] It is a homodimer and belongs to a subgroup of the jacalin-related lectin family that binds to glucose/mannose and presents two sugar-binding sites per monomer.

Although attempts at crystallization and further NMR experiments are presently being carried out in our laboratories, we have performed a preliminary docking analysis of the possible binding modes of **1**–**3** to BanLec.

First, the possibility of each saccharide simultaneously accessing the two binding sites of a given monomer was evaluated. For this, the different possible bound conformations deduced above from the trNOESY experiments in solution were considered.

From the X-ray structure of each of the monomers of BanLec complexed to two mannose moieties, the distance between the two O4 atoms of the bound sugars ranges between 13 and 14 Å.[20,21] For **1**, the distance between the O4 atoms of residues A and D oscillates between 7 and 11 Å, depending on the conformation around Φ and Ψ of both the 1→2 and 1→3 linkages. According to these numbers, it is not possible for one tetrasaccharide entity (or the trisaccharide) to be simultaneously bound to both binding sites. The possibility of docking each mannose residue to each of the two binding sites was then explored.

According to the AutoDock protocol, by considering the trNOESY-based bound conformation, that is, with all the 1→3 and 1→2 linkages in the negative Ψ region, the best solution shows that the tetrasaccharide is intimate with the Asp38 binding area of the lectin. The terminal non-reducing end occupies the position of the bound mannose,[20] giving the contacts already described for the monosaccharide, especially hydrogen bonds with Asp38 and van der Waals contacts with Phe131. The two residues ManB and ManC also provide sugar–protein contacts; Tyr83 (polar and non-polar contacts) and His84 hydrogen bond with ManC, whereas Asp35 establishes a hydrogen bond with ManB. There is a second available solution for which the second Man residue (ManB) replaces the bound Man in the crystal structure. In this case, Tyr83 establishes hydrogen bonds with both ManB and ManD, whereas His84 forms polar contacts with ManD. Thr61 interacts with ManA, Gly60, Lys91 Asp35 and Asp38 with ManB (Figure 5). According to the AutoDock calculations, Ψ torsion angles in the negative region preclude the recognition of the tetrasaccharide with the reducing end or ManC in this binding site. Moreover, the second binding site, in the vicinity of Gly15, cannot accommodate the tetrasaccharide with the NMR-derived bound geometry without major steric conflict (Figure 8 of the Supporting Information). Thus, two possibilities exist for BanLec to bind tetrasaccharide **1**, always in the same region and indeed with very similar contacts. In particular, the NMR results cannot distinguish between these two possible binding modes.

For the trisaccharide, docking of two different mannose residues of the 1→3 branch was attempted with either the gg or gt conformers at the 1→6 linkage. Both binding sites provided acceptable solutions, but only when the non-reducing mannose of the 1→3 arm interacted with the lectin. The major interactions were provided for ManA in both cases and, either for the interaction with Asp38 or Gly15

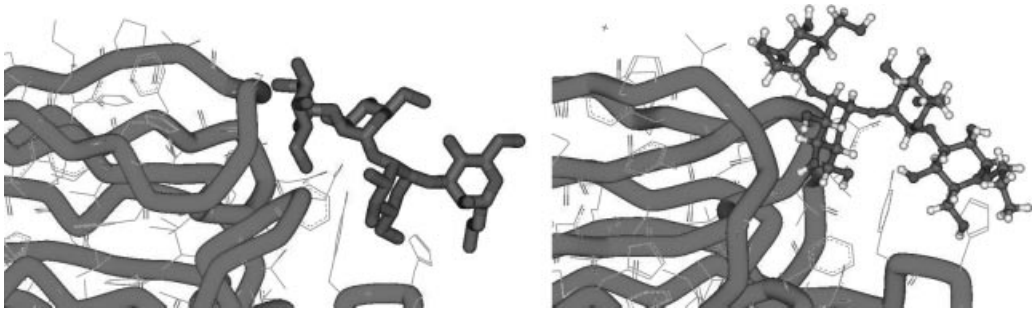

Figure 5. Representation of the two possible modes of interaction of tetrasaccharide **1** with banana lectin. Either the terminal non-reducing (left) or its contiguous Man moiety (right) of **1** may be docked at the Asp38 binding site without major steric conflict.

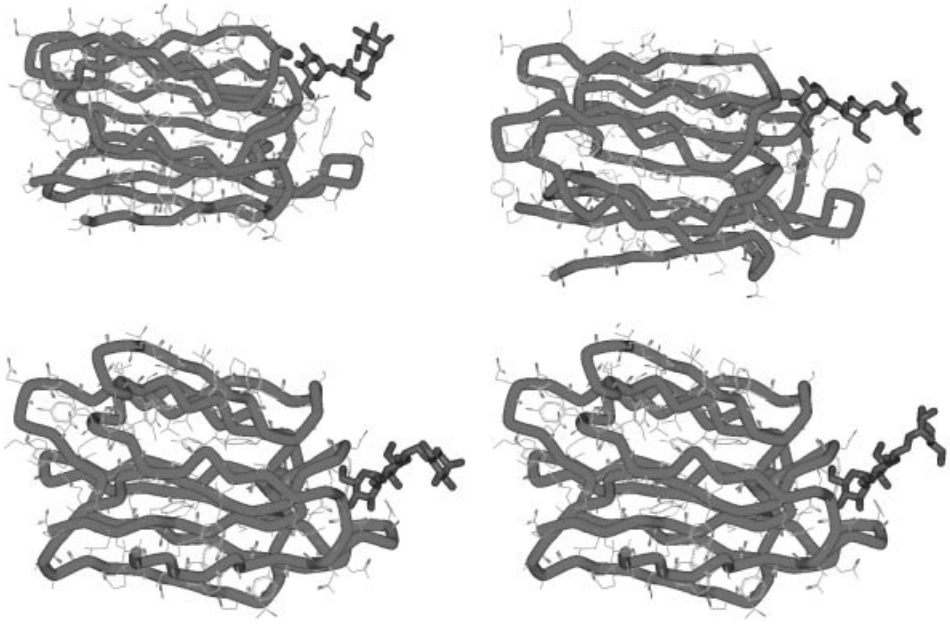

Figure 6. Docking of trisaccharide **2** at both banana lectin binding sites. The two non-reducing mannose moieties at the 1–3 arm could be docked with major steric conflict. Either the gg (left) or gt (right) rotamers at the 1–6 linkage are possible. In the top part, the D38 binding site is shown. In the bottom part, the G15 binding site is represented.

areas, both the gg or gt rotamers of mannose B were plausible. Indeed, no major contacts with the protein for this residue were evident from the docking solutions, giving rise to the possibility of simultaneous binding to the two Man binding sites.

For the heptasaccharide, taking into account the trNOESY-derived conformation with all the 1→2 linkages in the negative Ψ area (Figure 6), there is only one major solution from the AutoDock calculations and that displays a positive $\Psi_{1\rightarrow3}$ value (Figure 7). The complex obtained shows that the terminal Man residue of the 1→3 arm occupies the position of the Man residue at the Asp38 binding site. Binding at the Gly15 site using the experimental NMR geometry is not possible without major steric conflict. In the best solution, the three residues of the 1→3 arm, as well as the branching moiety, provide contacts with the protein similar to those described above for the first solution of the tetrasaccharide. Asp35, Asp38, Tyr83, His84 and Phe131 provide the intermolecular lectin–sugar hydrogen bonds and the van der Waals contacts required to stabilize the complex.[34,35]

Therefore, a combination of NMR methods and docking simulations has provided plausible solutions for the binding of these oligosaccharides to BanLec. Conformational selection processes take place in both the saccharide and lectin. For the smaller sugars, different binding modes of the saccharides to the same lectin probably occur. In any case, the NMR experiments reveal that the three oligosaccharides effectively interact with this lectin and that they may be used as recognition points in more complex multivalent synthetic systems. Further studies are taking place in our laboratories to explore these possibilities.

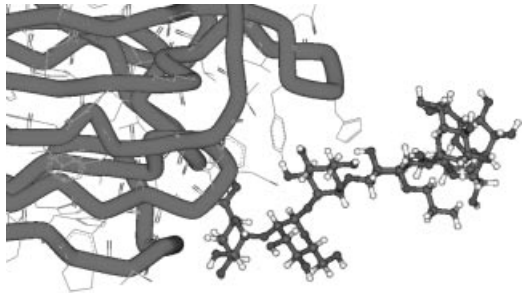

Figure 7. Representation of the best (AutoDock) mode of interaction of heptasaccharide **3** with banana lectin. The non-reducing moiety at the 1–3 arm of **3** may be docked at the Asp38 binding site without major steric conflict.

Experimental Section

Compounds: The oligosaccharides studied were prepared in good yields with a minimal number of building blocks according to the one-pot self-condensation synthesis described by Wong and coworkers.[36] The synthetic procedure will be reported elsewhere. Banana lectin was isolated and purified as described previously.[20]

NMR Spectroscopy: NMR spectra of compounds **1**–**3** were recorded in D_2O at 500 MHz with a Bruker AVANCE spectrometer at 298–300 K. The ^1H and ^{13}C NMR spectra of **1**–**3** were assigned employing a combination of 2D-TOCSY,[37] NOESY,[38] T-ROESY,[39] HSQC[40] and HSQC-TOCSY experiments. For studies of **1**–**3** in the free state, concentrations of 5 mM for **1** and **2**, and 3 mM for **3** were used.

The T-ROESY and NOESY experiments were performed in the phase-sensitive mode with the TPPI method for quadrature detection in *F*1. Typically, a data matrix of 2 k × 512 points was employed to digitise a spectral width of 4000 Hz. Between 32 and 48

scans were used per increment with a relaxation delay of 2 s. Prior to Fourier transformation, zero-filling was performed in *F*1 to expand the data to 4×2 k. Baseline correction was applied in both dimensions. The corresponding shift was optimized for the different spectra. In order to describe the conformational behaviour of **1**–**3**, selective 1D and 2D NOESY and T-ROESY experiments in D_2O were carried out.

These selective experiments were recorded employing a double-pulse field-gradient spin-echo (DPFGSE) module.[41] NOE intensities were normalised with respect to the diagonal peak at zero mixing time. Selective T_1 measurements were performed on the anomeric and several other protons to obtain the above-mentioned values. Experimental NOEs were fitted to a double exponential function, $f(t) = p_0(e^{-p_1 t})(1 - e^{-p_2 t})$, where p_0, p_1 and p_2 are adjustable parameters.[42] The initial slope was determined from the first derivative at time $t = 0$, $f'(0) = p_0 p_2$. From the initial slopes, interproton distances were obtained by employing the isolated spin-pair approximation (ISPA).

Chemical shifts and coupling constants are reported in the Supporting Information.

For the free molecules, NOESY cross peaks for the tetrasaccharide were slightly positive at room temperature, while those for the heptasaccharide were moderately negative. NOESY cross peaks for the trisaccharide were clearly positive.

For the bound ligand, trNOE experiments were performed as described previously[22] with a freshly prepared ligand/lectin solution. trNOESY experiments were then performed with mixing times of 50, 100, 200, 250 and 300 ms for an approximately 20:1 molar ratio of ligand/protein. For the three molecules a concentration between 2–3 mM of the ligand was employed. No purging spin-lock period was employed to remove the NMR signals of the macromolecule background as they were basically not observable owing to the large size of the receptor. First, line-broadening of the ligand protons was monitored after addition of the lectin. Strong negative NOE cross peaks were observed, in contrast to the free state, indicating binding of the sugars to the protein preparation. The theoretical analysis of the trNOEs of the sugar protons was performed using CORCEMA[27] and a relaxation matrix with exchange, as described previously.[33,35] Different exchange rate constants were employed to obtain the optimal match between experimental and theoretical results of the intra-residue cross peaks of the six-membered rings which have a relatively fixed geometry. The overall correlation time τ_c for the free state was always set to 0.18 ns for the trisaccharide, 0.25 ns for the tetrasaccharide and 0.5 ns for the heptasaccharide. τ_c for the bound state was set to 12 ns. To fit the experimental trNOE intensities, off-rate constants between 100 and 1000 s^{-1} were tested. Optimal agreement was achieved for k_{off} = 100–300 s^{-1}.

T-ROESY experiments were also carried out to exclude spin-diffusion effects. A continuous wave spin-lock pulse was used during the 250 ms mixing time. Key NOEs were shown to be direct cross peaks as they are opposite in sign to the diagonal peaks.[23]

STD experiments[43] were performed without saturation of the residual HDO signal for molar ratios between 15:1 and 50:1 of compound/protein. A series of Gaussian-shaped pulses of 50 ms each was employed with a total saturation time for the protein envelope of 2 s and a maximum *B*1 field strength of 60 Hz. An off-resonance frequency of δ = 40 ppm and on-resonance frequencies between δ = –1.0 and –2.0 ppm (protein aliphatic signals region) were applied. In all cases, line-broadening of the ligand protons was monitored.

Molecular Mechanics and Dynamics Calculations: Initial calculations for the free molecules were performed using the MacroModel/Batchmin[44] package (version 7.0) and the MM3* force field.[45] Charges were taken from the force field (all-atom charge option) and water solvation was simulated using MacroModel's generalized Born GB/SA continuum solvent model.[46]

The torsion angles Φ are defined as $H1_{ManA}$–$C1_{ManA}$–O–CX_{ManB} and Ψ as HX_{ManB}–CX_{ManB}–O–$C1_{ManA}$ for both 1→2 and 1→3 linkages. For the 1→6 linkage, Ψ is $C5_{Man}$–$C6_{Man}$–O–$C1_{Man}$. The torsion angle around the C5–C6 linkage (ω) is defined as O5–C5–C6–O6. Two different conformers were considered gt (ω = +60°) and gg (ω = –60°). The numbering of the different oligosaccharides is given in the corresponding schemes.[47] The GB/SA solvation model for water was used. The probability distribution was calculated from the energy values using the Boltzmann function at 300 K.

Docking Calculations: First, the different stable conformers of **1**, **2** and **3** were manually docked on both active binding sites of banana lectin by superimposing the terminal (reducing or non-reducing) residues of the corresponding tri- or heptasaccharide molecules on the existing mannose moieties of the two deposited Man/lectin and XylMan complexes (pdb codes, 1X1V and 2BN0, respectively, in ref.[20] and ref.[21]). For the tetrasaccharide, attempts were made to dock the four residues alternately at both binding sites. No minimisation was performed. Those solutions that led to steric hindrance or clashing were discarded.

Then the NMR-based solutions were used as input geometries for AutoDock 3.0 simulations[48] with the multiple Lamarckian Genetic Algorithm. The lectin coordinates were obtained (1X1V and 2BN0) from the Protein Data Bank.[49]

Grids of probe atom interaction energies and electrostatic potential were generated by the AutoGrid program present in AutoDock 3.0. Grid spacings of 0.6 and 0.375 Å were used for the global and local searches, respectively. For each calculation, 100 docking runs were performed using a population of 200 individuals and an energy evaluation number of 3×10^6.

Supporting Information (see footnote on the first page of this article): NMR spectra and conformational structures of **1**–**3** in the free and bound states. Chemical shifts of compounds **1** and **3**.

Acknowledgments

We thank the Ministry of Education and Science of Spain for funding grants (BQU2003-03550-C01) and grants from the Department of Science and Technology and the Department of Biotechnology, Government of India to A. S. We also thank Prof. N. R. Krishna (University of Birmingham, Alabama, USA) for the use of the CORCEMA programme for trNOESY analysis and to Dr. A. Olson (Scripps Research Institute, USA) for providing the AutoDock and auxiliary programs.

[1] H.-J. Gabius, H.-C. Siebert, S. Andre, J. Jimenez-Barbero, H. Rudiger, *ChemBioChem* **2004**, *5*, 740–764.
[2] Y. Ito, S. Matsuo, I. Hagihara, K. Totani, *Curr. Opin. Struct. Biol.* **2005**, *15*, 481–489.
[3] I. Botos, A. Wlodawer, *Prog. Biophys. Mol. Biol.* **2005**, *88*, 233–282.
[4] See, for instance: S. N. Lam, J. Gervay-Hague, *J. Org. Chem.* **2005**, *70*, 2387–2390.
[5] M. Mandal, V. Y. Dudkin, X. Geng, S. Danishefsky, *Angew. Chem. Int. Ed.* **2004**, *43*, 2557–2561.
[6] L. Kiessling, J. K. Pontrello, M. C. Schuster, "Synthetic multivalent carbohydrate ligands as effectors or inhibitors of bio-

logical processes" in *Carbohydrate-based drug delivery* (Ed.: C.-H. Wong), Wiley-VCH, Weinheim, **2003**, pp. 575–609.
[7] L. X. Wang, J. Ni, S. Singh, H. Li, *Chem. Biol.* **2004**, *11*, 127–134.
[8] a) A. G. Barrientos, J. M. De la Fuente, T. C. Rojas, A. Fernández, S. Penadés, *Chem. Eur. J.* **2003**, *9*, 1909–1921; b) J. M. De la Fuente, A. G. Barrientos, T. C. Rojas, J. Rojo, A. Fernández, S. Penadés, *Angew. Chem. Int. Ed.* **2001**, *40*, 2257–2261.
[9] See, for instance: a) A. C. de Souza, K. M. Halkes, J. D. Meeldijk, A. J. Verkleij, J. F. C. Vliegenthart, J. P. Kamerling, *ChemBioChem* **2005**, *6*, 828–831; b) J. Rojo, V. Díaz, J. de la Fuente, I. Segura, A. G. Barrientos, H. H. Riese, A. Bernad, S. Penadés, *ChemBioChem* **2004**, *5*, 291–297.
[10] H. Kogelberg, D. Solís, J. Jiménez-Barbero, *Curr. Opin. Struct. Biol.* **2003**, *13*, 646–653.
[11] J. M. De la Fuente, S. Penadés, *Biochim. Biophys. Acta* **2006**, *1760*, 636–651.
[12] D. D. Singh, K. Saikrishnan, P. Kumar, Z. Dauter, K. Sekar, A. Surolia, M. Vijayan, *Acta Crystallogr., Sect. D* **2004**, *60*, 2104–2106.
[13] I. J. Goldstein, *J. Agric. Food Chem.* **2002**, *50*, 6583–6585.
[14] R. J. Woods, A. Pathiaseril, M. R. Wormald, C. J. Edge, R. A. Dwek, *Eur. J. Biochem.* **1998**, *258*, 372–386.
[15] L. Gonzalez, D. Solis, T. Diaz-Mauriño, M. Bruix, M. Rico, T. Feizi, J. Jiménez-Barbero, *Arch. Biochem. Biophys.* **2000**, *383*, 17–27.
[16] A. Bernardi, A. Colombo, I. Sanchez-Medina, *Carbohydr. Res.* **2004**, *339*, 967–973.
[17] S. Mari, H. Posteri, G. Marcou, D. Potenza, F. Micheli, F. J. Canada, J. Jimenez-Barbero, A. Bernardi, *Eur. J. Org. Chem.* **2004**, 5119–5225.
[18] C. Clavel, A. Canales, G. Gupta, J. Cañada, S. Penadés, A. Surolia, J. Jiménez-Barbero, *Glycoconjugate J.*, submitted.
[19] C. J. Edge, U. C. Singh, R. Bazzo, G. L. Taylor, R. A. Dwek, T. W. Rademacher, *Biochemistry* **1990**, *29*, 1971–1974.
[20] D. D. Singh, K. Saikrishnan, P. Kumar, A. Surolia, K. Sekar, M. Vijayan, *Glycobiology* **2005**, *15*, 1025–1032.
[21] J. L. Meagher, H. C. Winter, P. Ezell, I. J. Goldstein, J. A. Stuckey, *Glycobiology* **2005**, *15*, 1033–1042.
[22] For a survey of NMR methods applied to saccharide molecules, see: J. Jiménez-Barbero, T. Peters, *NMR spectroscopy of glycoconjugates*, VCH, Weinheim, **2002**.
[23] For recent uses of STD in the carbohydrate field, see, for instance: V. Jayalakshmi, T. Biet, T. Peters, N. R. Krishna, *J. Am. Chem. Soc.* **2004**, *126*, 8610–8611.
[24] S. Mari, D. Serrano-Gómez, F. J. Cañada, A. L. Corbí, J. Jiménez-Barbero, *Angew. Chem. Int. Ed.* **2005**, *44*, 296–298.
[25] D. Neuhaus, M. P. Williamson, "The Nuclear Overhauser Effect" in *Structural and Conformational Analysis*, VCH, New York, **1989**.
[26] See, for instance: a) V. L. Bevilacqua, D. S. Thomson, J. H. Prestegard, *Biochemistry* **1990**, *29*, 5529–5537; b) V. L. Bevilacqua, Y. Kim, J. H. Prestegard, *Biochemistry* **1992**, *31*, 9339–9349.
[27] a) H. N. B. Moseley, E. V. Curto, N. R. Krishna, *J. Magn. Reson., Ser. B* **1995**, *108*, 243–261; b) N. R. Krishna, H. N. B. Moseley, *Biol. Magn. Reson.* **1999**, *17*, 223–307.
[28] T. J. Rutherford, J. Partridge, C. T. Weller, S. W. Homans, *Biochemistry* **1993**, *32*, 12715–12724.
[29] A. Almond, J. Duus, *J. Biomol. NMR* **2001**, *20*, 351–363.
[30] R. J. Woods, C. J. Edge, R. A. Dwek, *Nat. Struct. Mol. Biol.* **1994**, *1*, 499–501.
[31] A. Almond, J. Bunkenborg, T. Franch, C. H. Gotfredsen, J. O. Duus, *J. Am. Chem. Soc.* **2001**, *123*, 4792–4802.
[32] K. J. Naidoo, D. Denysyk, J. W. Brady, *Environ. Prot. Eng. Prot. Eng.* **1997**, *10*, 1249–1261.
[33] Concanavaline A also shifts the conformational distribution of the *C*-glycosyl analogue of **2**, see: L. M. Mikkelsen, M. J. Hernáiz, M. Martín-Pastor, T. Skrydstrup, J. Jiménez-Barbero, *J. Am. Chem. Soc.* **2002**, *124*, 14940–14951.
[34] For the importance of aromatic–sugar interactions, see, for instance: M. C. Fernández-Alonso, F. J. Cañada, J. Jiménez-Barbero, G. Cuevas, *J. Am. Chem. Soc.* **2005**, *127*, 7379–7386.
[35] For a similar docking analysis of a carbohydrate to a lectin, see: J. L. Asensio, J. F. Espinosa, H. Dietrich, F. J. Cañada, R. R. Schmidt, M. Martin-Lomas, S. André, H.-J. Gabius, J. Jiménez-Barbero, *J. Am. Chem. Soc.* **1999**, *121*, 8995–9000.
[36] H.-K. Lee, C. N. Scanlan, C.-Y. Huang, A. Y. Chang, D. A. Calarese, R. A. Dwek, P. M. Rudd, D. R. Burton, I. A. Wilson, C.-H. Wong, *Angew. Chem. Int. Ed.* **2004**, *43*, 1000–1003.
[37] A. Bax, D. G. Davis, *J. Magn. Reson* **1985**, *65*, 355–360.
[38] A. Kumar, R. R. Ernst, K. Wüthrich, *Biochem. Biophys. Res. Commun.* **1980**, *95*, 1–6.
[39] T. L. Hwang, A. J. Shaka, *J. Am. Chem. Soc.* **1992**, *114*, 3157–3158.
[40] G. Bodenhausen, D. J. Reuben, *Chem. Phys. Lett.* **1980**, *69*, 185–189.
[41] K. Stott, J. Stonehouse, J. Keeler, T. L. Hwang, A. J. Shaka, *J. Am. Chem. Soc.* **1995**, *117*, 4199–4200.
[42] See, for instance: J. L. Asensio, F. J. Cañada, N. Khan, D. A. Mootoo, J. Jiménez-Barbero, *Chem. Eur. J.* **2000**, *6*, 1035–1041.
[43] M. Mayer, B. Meyer, *J. Am. Chem. Soc.* **2001**, *123*, 6108–6117.
[44] F. Mohamadi, N. G. J. Richards, W. C. Guida, R. Liskamp, M. Lipton, C. Caufield, G. Chang, T. Hendrickson, W. C. Still, *J. Comput. Chem.* **1990**, *11*, 440–467.
[45] N. L. Allinger, Y. H. Yuh, J. H. Lii, *J. Am. Chem. Soc.* **1989**, *111*, 8551–8566.
[46] W. C. Still, A. Tempzyk, R. Hawley, T. Hendrickson, *J. Am. Chem. Soc.* **1990**, *112*, 6127–6129.
[47] For the application of molecular mechanics force fields to the conformational analysis of carbohydrate molecules, see: S. Perez, A. Imberty, S. Engelsen, J. Gruza, K. Mazeau, J. Jimenez-Barbero, A. Poveda, J. F. Espinosa, B. P. van Eyck, G. Johnson, A. D. French, M. Louise, C. E. Kouwijzer, P. D. J. Grootenuis, A. Bernardi, L. Raimondi, H. Senderowitz, V. Durier, G. Vergoten, K. Rasmussen, *Carbohydr. Res.* **1998**, *314*, 141–155.
[48] G. M. Morris, D. S. Goodsell, R. S. Halliday, R. Huey, W. E. Hart, R. K. Belew, A. J. Olson, *J. Comput. Chem.* **1998**, *19*, 1639–1647.
[49] The Protein Data Bank (www.rcsb.org/pdb): H. M. Berman, J. Westbrook, Z. Feng, G. Gilliland, T. N. Bhat, H. Weissig, I. N. Shindyalov, P. E. Bourne, *Nucleic Acids Res.* **2000**, *28*, 235–242.

Received: October 13, 2006
Published Online: February 9, 2007

